NeuroImage 111 (2015) 580–589

Contents lists available at ScienceDirect

NeuroImage

journal homepage: www.elsevier.com/locate/ynimg

Longitudinal measurement of the developing grey matter in preterm subjects using multi-modal MRI

Zach Eaton-Rosen [a,*], Andrew Melbourne [a], Eliza Orasanu [a], M. Jorge Cardoso [a], Marc Modat [a], Alan Bainbridge [b], Giles S. Kendall [c], Nicola J. Robertson [c], Neil Marlow [c], Sebastien Ourselin [a]

[a] Translational Imaging Group, CMIC, UCL, UK
[b] Medical Physics, University College Hospital, London, UK
[c] Academic Neonatology, EGA UCL Institute for Women's Health, London, UK

ARTICLE INFO

Article history:
Accepted 5 February 2015
Available online 12 February 2015

ABSTRACT

Preterm birth is a major public health concern, with the severity and occurrence of adverse outcome increasing with earlier delivery. Being born preterm disrupts a time of rapid brain development: in addition to volumetric growth, the cortex folds, myelination is occurring and there are changes on the cellular level. These neurological events have been imaged non-invasively using diffusion-weighted (DW) MRI. In this population, there has been a focus on examining diffusion in the white matter, but the grey matter is also critically important for neurological health. We acquired multi-shell high-resolution diffusion data on 12 infants born at ≤28 weeks of gestational age at two time-points: once when stable after birth, and again at term-equivalent age. We used the Neurite Orientation Dispersion and Density Imaging model (NODDI) (Zhang et al., 2012) to analyse the changes in the cerebral cortex and the thalamus, both grey matter regions. We showed region-dependent changes in NODDI parameters over the preterm period, highlighting underlying changes specific to the microstructure. This work is the first time that NODDI parameters have been evaluated in both the cortical and the thalamic grey matter as a function of age in preterm infants, offering a unique insight into neuro-development in this at-risk population.

Introduction

Rates of preterm birth have risen over the past 20 years in developed nations (Beck et al., 2010). Due to advances in medical practice and technology, infants survive this period more often; however preterm birth remains the leading cause of neonatal mortality and associated morbidity often persists into adulthood. Disabilities linked with preterm birth are among the most pressing public health concerns in Europe and the U.S.A. (Behrman and Butler, 2007). Very preterm infants (≤32 weeks of completed gestation) are significantly more likely to suffer from cerebral palsy, cognitive deficits, loss of neuro-motor function and have long-term difficulties in education (Saigal and Doyle, 2008). Extremely preterm infants (≤25 weeks of completed gestation) have rates of 49% for disability and 23% for severe disability (Wood et al., 2000). There are extensive costs associated with the extended perinatal care and ongoing support into adulthood (Petrou, 2003). Research into this population is necessary in order to predict the likelihood of specific deficits and compare different early intervention strategies.

The preterm period is critical for neuro-development. As well as increases in brain volume, the cortex folds and on the cellular level, neural afferents and glia travel radially to populate the cortex (Bystron et al., 2008). These changes cannot be imaged using conventional MRI, as the length scales of changes are orders of magnitude below currently attainable resolution. Diffusion-weighted MRI (DW MRI) is a non-ionising, non-invasive technique that is sensitive to cytoarchitecture on the scale of microns (Le Bihan, 2003). The signal is sensitised to the bulk molecular motion of water in a given magnetic gradient direction. By sampling a variety of gradient directions, we establish how the water preferentially diffuses within a voxel. Water diffuses differently depending on local conditions and so, by fitting models to the diffusion signal, we infer something about the microstructure. One popular model uses a 'diffusion tensor' (DT) to model diffusion as taking place ellipsoidally (Basser et al., 1994). In regions of homogeneous and aligned white matter, these ellipsoids are highly oblate (cigar-like), whereas they would be spheroidal in the cerebro-spinal fluid (CSF) where diffusion is unconstrained and isotropic. Measures such as the Fractional Anisotropy (FA) summarise properties of the tensor — in this case, how isotropic the distribution is (Basser, 1995). The mean diffusivity (MD) represents the average diffusivity of the tensor. The FA and other scalars derived from the tensor depend, in a complex way, on the local microstructure.

DTI measures have been characterised during developmental sequences (Dubois et al., 2008) — FA tends to increase throughout the

* Corresponding author.
E-mail address: zach.eaton-rosen.12@ucl.ac.uk (Z. Eaton-Rosen).

http://dx.doi.org/10.1016/j.neuroimage.2015.02.010

perinatal period in white-matter regions (Partridge et al., 2004). DTI parameters show correlations with disabilities associated with preterm birth (Ment et al., 2009) and the pattern of deficits forms a recognisable 'amalgam' of effects (Volpe, 2009). In the cortex, the elaboration of the radial glial cells causes a drop in the FA as radial diffusivity decreases due to the cellular maturation (McKinstry et al., 2002). Recent work has attributed the changes in DTI parameters to a general increase in complexity (Ball et al., 2013). This work also showed that diffusion parameters for preterm infants depend on how preterm the infant is at birth.

Developmental changes are also seen in the thalamus, a deep grey matter structure acting as a major relay centre for communication with the cerebral cortex. In the preterm period, thalamo-cortical connectivity is developing, underpinning basic cognitive processes, including the development of sensory perception (Kostović and Judas, 2010). The early preterm population is especially susceptible to sensory impairments, including in hearing and vision (Wood et al., 2000). These deficits may have correlates in the imaging data. MRI measurements of reduced thalamic volume have been shown to correlate with later disability (Ball et al., 2012). The developmental importance of the thalamus and thalamo-cortical connections suggests that non-invasively measuring its growth, both in volume and microstructure, will have predictive value for future outcome.

Despite the successes of DTI, it remains challenging to attribute changes in parameters to specific microstructural changes (Trivedi et al., 2009). Bulk measures such as FA conflate several effects: a low FA measurement could be due to partial volume effects with CSF, fibre dispersion, the cellular density changing or a change in myelination state. A promising line of investigation into diffusion properties relies on acquiring data at more b-values and gradient directions. At different b-values, the signal reduces at different rates depending on the local environment. Acquiring such data allows multi-compartment models to be fitted. One early example of these models used multiple pools, with exchange, to model the diffusion of water (Stanisz et al., 1997). These models are based on the underlying structure of the tissue and so interpretation of the signal is more directly related to the underlying structure. More recent models have simplified many of the assumptions — for example by ignoring exchange. In the CHARMED model, compartments include intra- and extra-axonal spaces (Assaf and Basser, 2005). These models tend to require a thorough diffusion acquisition at high angular resolution and a wide range of b-values. The full CHARMED acquisition is unsuitable for the neonatal population because of the acquisition duration.

The Neurite Orientation Dispersion and Density Imaging model (NODDI) (Zhang et al., 2012) is a multi-compartment microstructural model for multi-shell diffusion data. The model can be fitted with only two 'shells' of diffusion data because of some simplifying assumptions. This model has been used to investigate the white matter of infants shortly after birth (Kunz et al., 2014). This demonstrated that the maturation state of different white matter regions could be separated by using the NODDI parameters in addition to the FA measurement. Counsell et al. have demonstrated NODDI parameter changes in the thalamus during early infancy (Counsell et al., 2014). Because NODDI is a unified model for both the grey-matter and the white-matter, it is suitable for the current study.

NODDI divides the diffusion signal into coming from compartments of v_{iso}, v_i and v_e. v_{iso}, the isotropic volume fraction, represents water diffusing isotropically with the diffusivity of free water, as in the fluid-filled ventricles or the cerebrospinal fluid. The intra-neurite volume fraction, v_i, represents how much of the remaining space is occupied by the neurites. Water diffuses preferentially along the length of the neurites. As well as defining the angles of anisotropy, this compartment is dispersed by an amount determined by the Orientation Dispersion Index (ODI). Small values of this represent tightly-aligned diffusion. Finally, the extra-neurite environment, v_e, is categorised by diffusion hindered perpendicular to the neurites. The mathematical details are explained in the Neurite Orientation Dispersion and Density Imaging (NODDI) section.

Longitudinal changes in the brain, as measured by MRI, may have important cognitive correlates. In the presented work, we calculate changes in diffusion parameters in the grey matter. We combine state-of-the-art signal modelling and image processing in order to derive how these microstructural parameters coincide with known developmental processes. These sensitive measures may aid in predicting patient outcomes in this at-risk population.

In this work we extend our work in this domain (Eaton-Rosen et al., 2014a, 2014b) by establishing normative NODDI values for the preterm population in the cortex and thalamus, and quantifying microstructural, longitudinal changes over the preterm period.

Hypothesis

DTI changes in the cortex are related to growth of dendrites and other microstructural changes (McKinstry et al., 2002). This hinders diffusion, reflected by reductions in MD and in FA (Ball et al., 2013). We predict that this change will manifest as an increased ODI over the preterm period, because the diffusion becomes more dispersed as the dendrites and axons are elaborated. We also predict v_i to rise because of increasing density. In terms of v_{iso}, we know that the water content in the brain is decreasing, and thus the diffusivity will also decrease. Therefore, as the diffusivity becomes farther from the value for free water, v_{iso} will decrease.

The nucleic substructures of the thalamus have formed by 24 weeks of gestation (Dekaban, 1954). Thus, we expect the fibres to retain similar geometry, and hence similar ODI between the timepoints. There is a decrease in radial diffusivity (Ball et al., 2012) which is related to the histological knowledge that the thalamus is myelinating during the preterm period (Hasegawa et al., 1992). In other studies using NODDI to explore white matter characteristics in newborns, it was shown that v_i is related to the myelination status in the posterior limb of the internal capsule (Kunz et al., 2014). Therefore, we would expect an increase in v_i in the thalamus over the preterm period. This increase was noted in Counsell et al. (2014). We expect v_{iso} to be small at both timepoints.

Methods

Subjects

From February 2012 to March 2014, 28 infants were recruited for the study. Infants were excluded if they had abnormal cerebral ultrasound, or if either the diffusion acquisition or the structural acquisition was unusable due to patient movement. Twelve infants were included with mean estimated gestational age (EGA) of 25.9 ± 1.0 weeks at birth. Seven of these had the full data acquisition at pre- and full-term timepoints, so there were 19 sets of scans in total. All infants in this study were born at <28 weeks of completed gestation and their characteristics are summarised in Table 1. Informed parental consent was obtained for all infants and the study was approved by the local research ethics committee.

MR acquisitions

We acquired MRI data on a Philips Achieva 3 T MRI machine. The infants were imaged when spontaneously asleep after feeding, without sedation, in an MR-compatible incubator.

The T_1-weighted scans used a 3D MP-RAGE at a resolution of $0.82 \times 0.97 \times 1.0$ mm (reconstructed to $0.82 \times 0.82 \times 0.5$ mm) at T_R / T_E = 17/4.6 ms, acquisition duration 462 s.

The diffusion-weighted sequence had 54 diffusion directions — 6 reference volumes at b = 0 smm^{-2}, 16 at b = 750 smm^{-2} and 32 at b = 2000 smm^{-2}. Resolution was acquired at $2.0 \times 2.0 \times 2.0$ mm and reconstructed to $1.75 \times 1.75 \times 2.00$ mm^3. T_R was 9 s and T_E was 60 ms, with a total acquisition time of 703 s.

Table 1
This table presents the subjects in the experiment. *s and †s denote twins. N/A refers to missed scans (d, k at preterm) or scans that haven't yet taken place (l at term). The column '%D' refers to the percentage of diffusion-weighted scans that were included after diffusion pre-processing.

Subject identifier	EGA at birth (weeks, days)	Birth weight (grams)	Sex	EGA at scan 1	Quality control (QC)	%D	EGA at scan 2	QC	%D
a	26 + 1	784	M	33 + 1	Yes	93	40 + 1	Yes	93
b*	26 + 4	903	M	34 + 2	T_1 motion	N/A	48 + 2	Yes	98
c*	26 + 4	922	M	34 + 2	T_1 motion	N/A	48 + 2	Yes	89
d	25 + 2	776	M	N/A	N/A	N/A	37 + 4	Yes	91
e†	25 + 1	730	M	31 + 3	Yes	94	42 + 0	Yes	98
f†	25 + 1	760	F	31 + 0	Yes	83	42 + 0	Yes	91
g**	27 + 1	1038	M	30 + 6	Yes	94	46 + 2	Yes	93
h**	27 + 1	880	F	29 + 6	Yes	94	46 + 2	Yes	80
i‡	26 + 2	940	M	31 + 6	Yes	91	40 + 2	Yes	100
j‡	26 + 2	1095	M	34 + 4	Yes	46	40 + 2	Yes	80
k	23 + 6	680	M	N/A	N/A	N/A	38 + 6	Yes	67
l	25 + 4	956	M	27 + 3	Yes	93	N/A	N/A	N/A

Because of the level of subject movement, it was necessary to use a scanning sequence that is economical in terms of time. Our two-shell diffusion sequence is performed over a short timescale and thus is suitable for this population.

Neurite Orientation Dispersion and Density Imaging (NODDI)

NODDI (Zhang et al., 2012) is a multi-compartment model for DW signal acquired at multiple b-values. There are 5 free parameters in NODDI: two angles, v_{iso}, v_i and the ODI. The diffusivities are fixed. The signal, $A(bval = b, bvec = \mathbf{q})$, is given by:

$$A(b, \mathbf{q}) = v_{iso}A_{iso} + (1-v_{iso})(v_iA_i + (1-v_i)A_e). \quad (1)$$

In the isotropic volume fraction, v_{iso}, water diffuses isotropically with a diffusivity of $d_{iso} = 3.00 \times 10^{-3}$ mm^2 s^{-1}, the value for free water. $A_{iso} = e^{-bd_{iso}}$.

The remaining volume is divided into v_i and $(1 - v_i) = v_e$: respectively, the volume fractions of intra- and extra-neurite compartments. Diffusion in neurites is modelled with cylinders of zero radius with diffusivity in the axial direction set to 2.00×10^{-3} mm^2 s^{-1}. This value is higher than that for adult subjects and is set to the same value as Kunz et al. (2014). The sticks are dispersed by a Watson distribution as in Zhang et al. (2011), with the orientation dispersion index ($0 \leq ODI \leq 1$) representing how dispersed this diffusion is. $A_{ic} = \int_{S^2} f(\mathbf{n}) e^{-bd_{||}(\mathbf{q}\cdot\mathbf{n})^2} d\mathbf{n}$ where $f(\mathbf{n})$ is given by the Watson distribution: $f(\mathbf{n}) = M\left(\frac{1}{2}, \frac{3}{2}, \kappa\right)^{-1} e^{\kappa(\mu\cdot\mathbf{n})^2}$, where M is a confluent hypergeometric function and μ is the mean orientation. κ is related to the ODI as $\kappa = 1/\tan\frac{\pi * ODI}{2}$.

For the results in this paper, the values labelled 'v_i' are actually $(1 - v_{iso})v_i$. This is so that the parameter value refers to the proportion of the voxel being taken up by intra-neurite space. It is worth noting that v_{iso} values are near zero in most WM and GM tissues.

The extra-neurite volume fraction, v_e, uses an anisotropic Gaussian diffusion model to represent the space around the neurites. This represents the water being hindered by the presence of neurites, preferentially diffusing parallel to them. It is also dispersed by the ODI. $\log A_e = -b\mathbf{q}^T\left(\int_{S^2} f(\mathbf{n}) D(\mathbf{n}) d\mathbf{n}\right)\mathbf{q}$.

NODDI has similarities with the CHARMED model, such as the volume fractions. While CHARMED has a minimum of twelve free parameters per voxel (Assaf and Basser, 2005), a reduced version, CHARMED-light, has been proposed and compared with the NODDI model's parameter estimates. The volume fractions were similar in the white matter of neonates (Kunz et al., 2014). The NODDI model has the advantage of modelling grey and white matter, and has added information about the dispersion in the diffusion. These measurements may highlight the dynamics of cortical and other grey matter maturation. This unified model for brain tissue is suited to the quickly changing microstructural landscape of the infant brain.

We fitted the model by non-linear least squares after initialising using the diffusion tensor model and a grid search, using the NODDI Matlab Toolbox.[1]

Diffusion preprocessing

An underlying assumption of fitting a diffusion model is that a voxel's signal comes from the same place in the anatomy. For bulk motion during the protocol, common in the neonatal population, there will be displacement in the images which can be corrected by registration. If a subject moves during an acquisition, there is significant signal dropout. We manually identify affected volumes by their signal dropout and remove them. Imaging artefacts can also cause errors in alignment which also require correction.

To align the images we adopt an image registration strategy inspired by Bai and Alexander (2008). Affine registration to reference volumes ameliorates eddy-currents as well as correcting for bulk motion. While some techniques register to the reference ($b = 0$) values, this means that the contrast in reference and floating images are drastically different. To register to a target with a similar contrast, we generate 'synthetic' reference images. Our pre-processing algorithm is presented in Fig. 1 and achieves this in three steps. After bad volumes are removed (1), each volume is registered to the groupwise average of all of the $b = 0$ images (2). We then fit the diffusion tensor model and use the model to produce synthetic images, for each b-value and gradient direction. Each raw image is then registered affinely to its synthetic partner (3). Because these were constructed after registration to the $b = 0$ images, registering these can simultaneously correct for distortion and motion between acquisitions. From the transformations, we rotated the b-vectors and modulated the image intensities by the Jacobian determinant (Jones et al., 2013), assuming that the largest part of the rotation in the affine transformation was due to bulk motion (Leemans and Jones, 2009). All registrations are carried out using NiftyReg (Ourselin et al., 2000, 2002).

Segmentation

In order to analyse the NODDI parameter maps, we require anatomical labels in the diffusion space. Image segmentation is difficult in neonates for reasons including poor image contrast, lower SNR, the increased prevalence of motion artefacts and patient heterogeneity. The smaller size of the brain, compared to adults, also means that partial volume effects are more common. To avoid directly segmenting the

[1] http://www.nitrc.org/projects/noddi_toolbox.

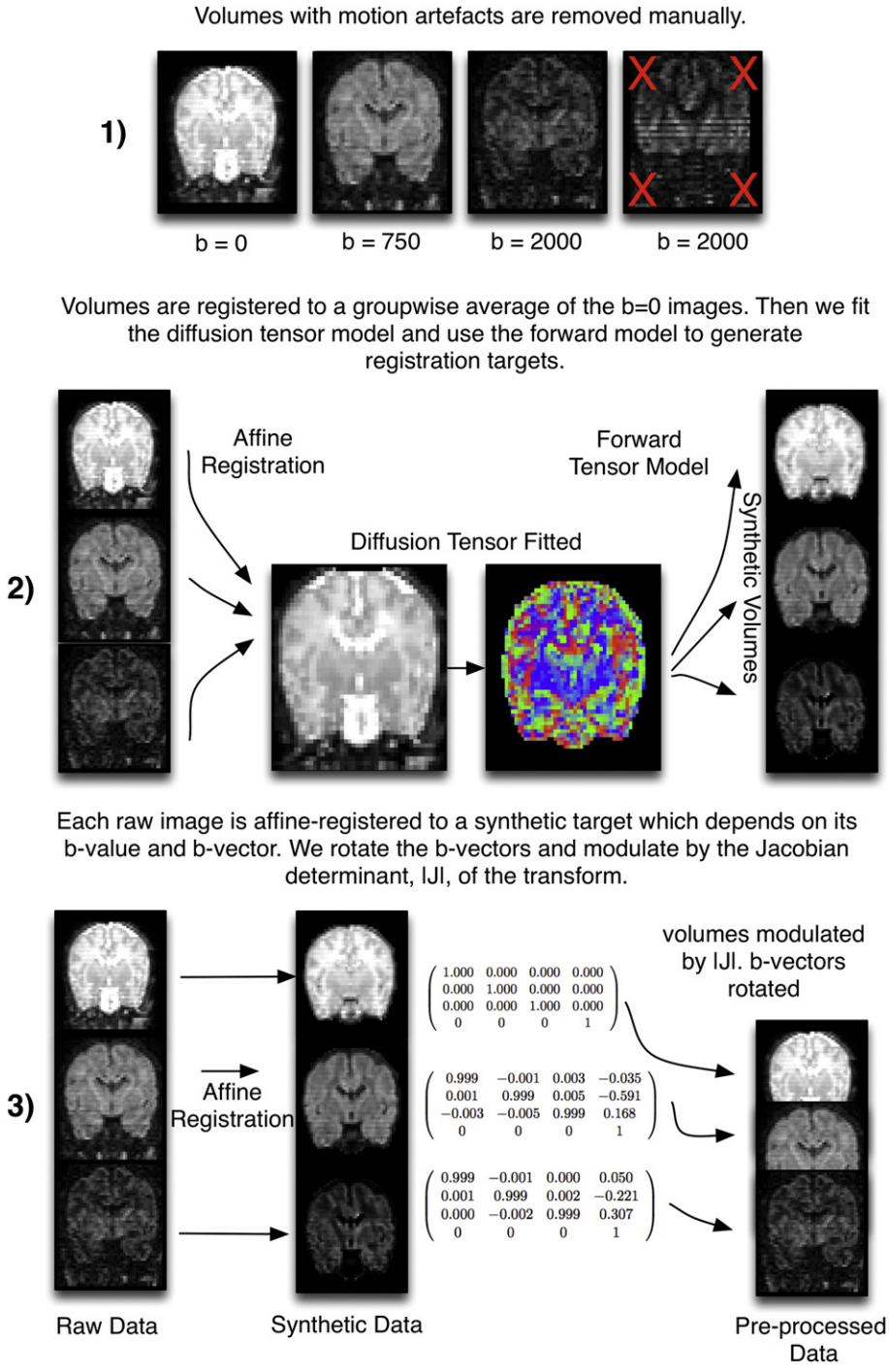

Fig. 1. The pre-processing pipeline. High b-value images have markedly different contrast from the b = 0 images. Thus, to ensure that each image has a suitable registration target, we generate these using the diffusion-tensor model. We use the forward model to generate the registration targets.

diffusion images, we segment the T_1 weighted images and propagate the labels into diffusion space. Here we outline our approach.

To segment the T_1-weighted structural images, we used the AdaPT algorithm (Cardoso et al., 2013) which is optimised for a preterm subject group. It uses a probabilistic Gaussian mixture model, initialised with a 6-class 4-D probabilistic atlas specific to the neonatal population (Kuklisova-Murgasova et al., 2011). We manually corrected brain masks in order to initialise the segmentation. The tissue classes are: white matter (WM), cortical grey matter, cerebellum, deep grey matter, cerebrospinal fluid (CSF) and brainstem. In order to segment the thalamus, we used segmentation propagation (Cardoso et al., 2012) to fit a population-specific neonatal atlas (Gousias et al., 2012) to the T_1-weighted data, generating a 50-label map for each subject from which we took the thalamus. The segmentations for the longitudinal infants at preterm and term timepoints are shown in Fig. 2.

We registered the T_1 to diffusion space rigidly and propagated the segmentation. However, because diffusion images have magnetic susceptibility artefacts, the true transformation is non-linear in nature. Susceptibility distortions occur in regions of high differential in magnetic susceptibility, such as the occipital and frontal cortices (Greve and Fischl, 2009). It is important to note that on deforming the diffusion space to its correct anatomical dimensions, the diffusion information from each voxel

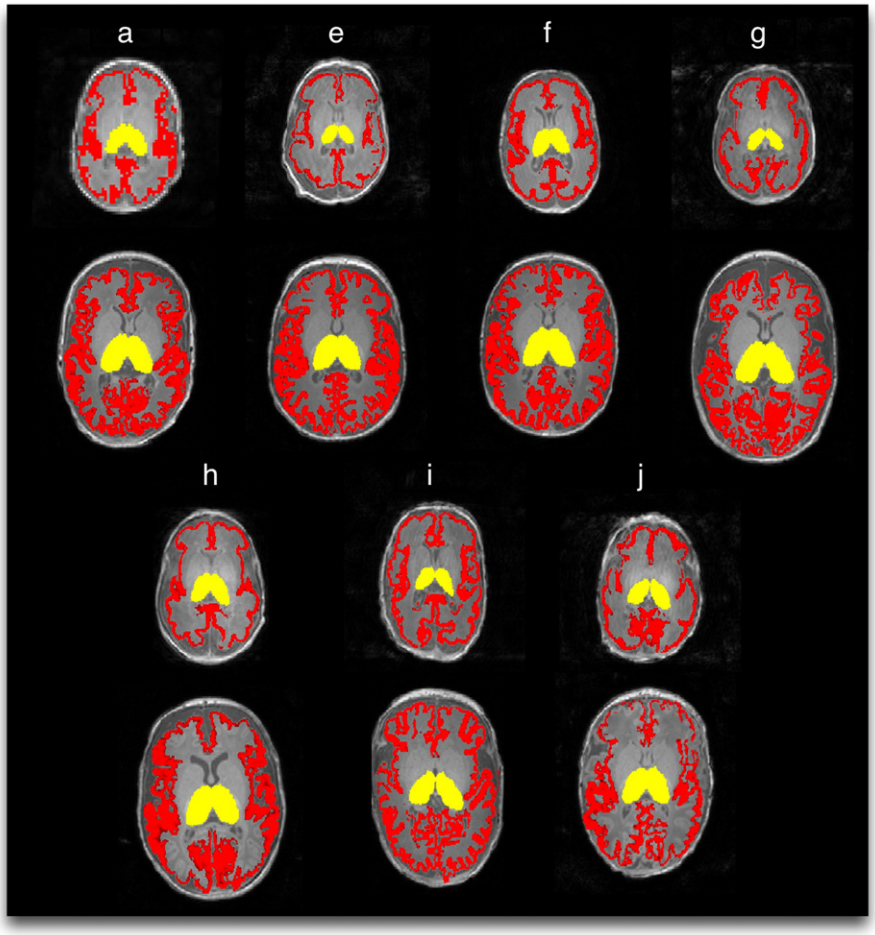

Fig. 2. The segmentations at preterm (top) and term (bottom) timepoints of the thalamus (yellow) and the cortex (red).

cannot be retrieved. The susceptibility artefact means that many voxels' signal is compressed into fewer, leading to characteristic bright regions. This signal effectively averages across several voxels, which will span multiple tissue classes. Therefore it is important to disregard these areas in the analysis.

To identify regions of susceptibility distortion for exclusion, we compare the tissue segmentation in diffusion space to the MD map. The MD has good contrast for the CSF/cortex boundary and so we identify slices where the segmentation fits poorly by examining the segmentation overlaid on the MD image. We manually edit the masks to exclude the regions of the cortex where the segmentation is incorrect, which has been caused by susceptibility distortion. Doing this, the major deformations are especially prevalent in the occipital and frontal cortices as expected (Greve and Fischl, 2009). We show an example where the excluded regions are highlighted (Fig. 3). We also exclude voxels from the analysis where v_{iso} exceeds 50% because this implies that the tissue label for this voxel is wrong.

Cortex and partial volume

For the infants in our study, the cortical layer is 1–2 mm thick. Thus, due to the voxel size, there will be significant partial volume effects in the cortical region. It is unlikely that the observed parameters will reflect only the changes in the cortex. However, the v_{iso} component, in principle, will remove the effects of isotropic diffusion, for example at the cortex–CSF boundary. In the WM–GM regions, the fit will model diffusion data coming from both tissue types.

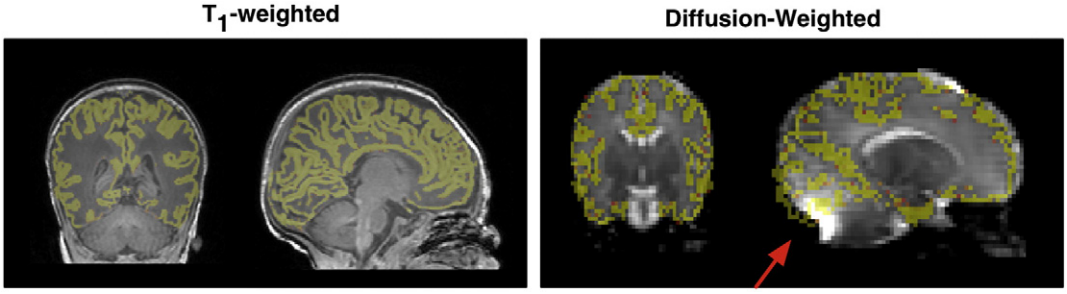

Fig. 3. The segmentations still fit well in most cortical regions after being registered to diffusion space. However, in regions with susceptibility distortion (arrow) there is a shift in cortical boundary. Diffusion signal in this region comes from a greater range of locations in physical space. We manually exclude the regions that fall outside of the brain in the diffusion image.

Results

Parameter maps

We fitted the NODDI and DTI models for each infant brain (Figs. 4, 5). The FA maps show the expected pattern of contrasts, with high values in the cortex at the preterm timepoint. This high-anisotropy rim is no longer apparent by term-equivalent age. The MD is high in regions of CSF. In terms of NODDI parameters, the v_{iso} component is high in regions of the cerebrospinal fluid — outside of the brain and in the ventricles. Well defined and highly-directional white matter areas, such as the corpus callosum (CC), tend to have the highest v_i values, in both 30- and 40-week scans. The v_i values in the cortex are lower than in the CC but appear as high-value regions compared to the adjoining white matter. There is a general increase in contrast over the preterm period. ODI is low in the corpus callosum and white matter projection tracts. At the term timepoint, the cortex has greater contrast from surrounding matter than at the preterm timepoint. By excluding voxels in which $v_{iso} > 0.5$, the cortex had 8% (pre) and 4% (term) of voxels removed while the thalamus had 3% (pre) and 2% (term).

Cortical results

We combined the data from all longitudinal subjects for analysis. The histograms of the parameters at term and preterm timepoints are shown in Fig. 6. We reproduce the result that the FA and MD both decrease over the preterm period (Ball et al., 2013). With the NODDI model, these changes manifest predominantly as changes in the ODI. Fitting a normal distribution to these histograms, the mean of the ODI increases from 0.298 ± 0.001 to 0.436 ± 0.001 (note that these errors are the 95% confidence interval for the mean after fitting a Gaussian, not the standard deviation of the distribution). The v_i has a small change, from 0.231 ± 0.001 to 0.239 ± 0.001. We also plotted results individually for each infant summarised in these graphs, in Supplementary Figs. 8 and 9.

Thalamus results

Fig. 6 displays the histograms for the thalamus. In the thalamus, the MD decreases and the FA increases during the preterm period, as in Ball et al. (2012). There is an increase in v_i from 0.241 ± 0.001 to 0.312 ± 0.001. The ODI remains constant — from 0.344 ± 0.003 to 0.342 ± 0.002. We also plotted results individually for the thalamic GM in Supplementary Fig. 9.

Cross-sectional analysis

To include the data from infants with only one timepoint with the longitudinal subjects, we plotted the means of the parameters as a function of gestational age (Fig. 7). The confidence intervals on the mean were calculated by assuming a normal distribution on the parameters, which is supported by visual inspection (Fig. 6).

In Fig. 7 we can see that the trends represented by the histograms seem to hold for the subject pool as a whole. To analyse the trends,

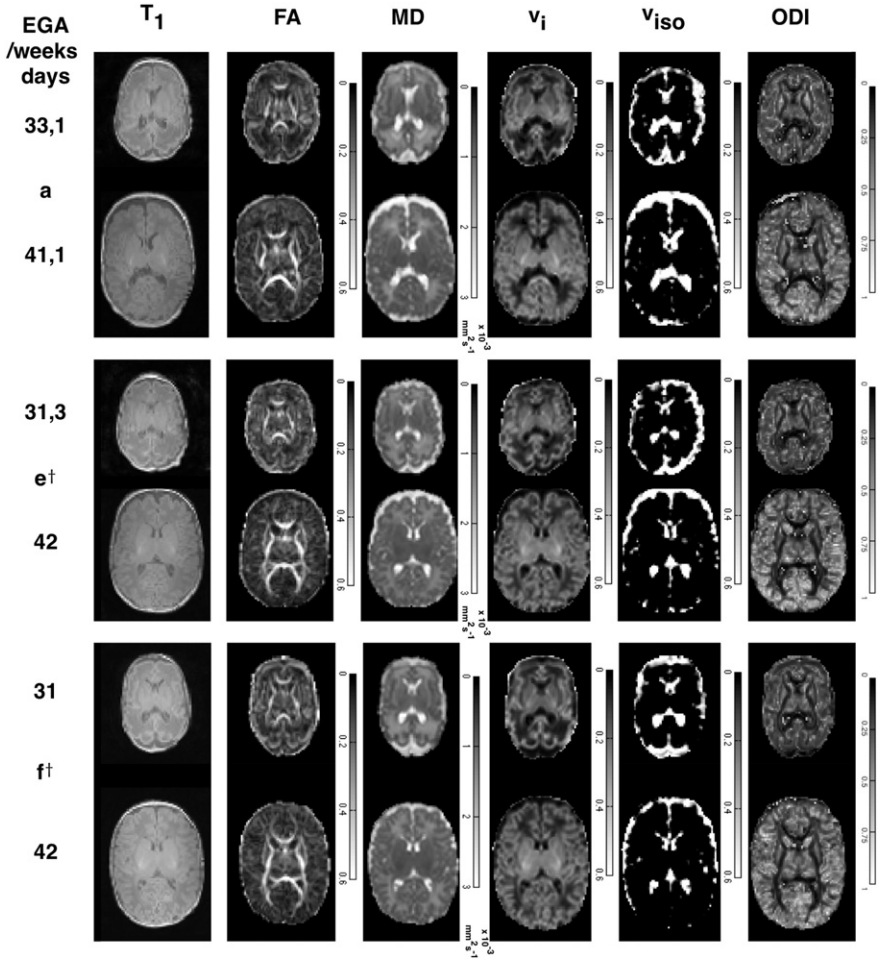

Fig. 4. Parameter maps for infants at preterm and term timepoints.

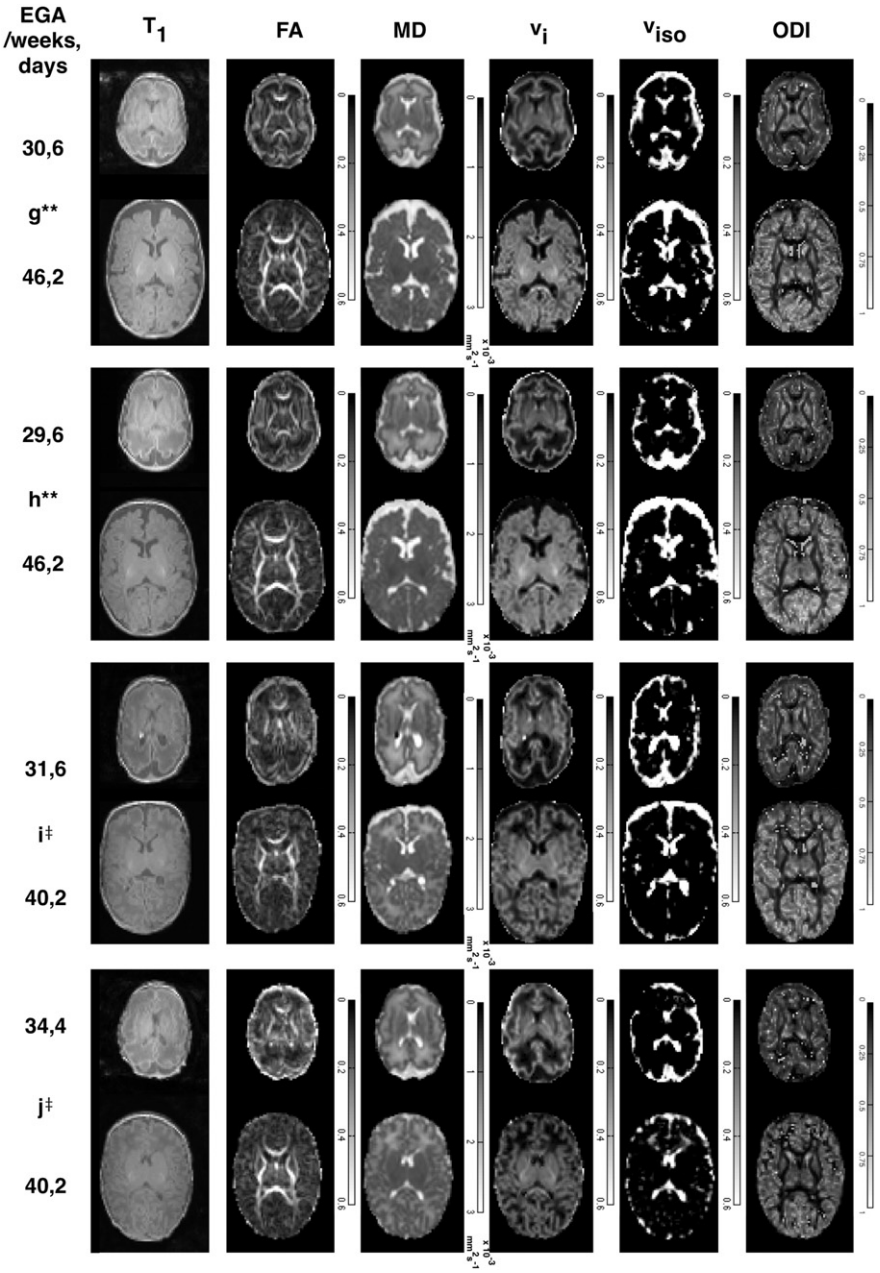

Fig. 5. Parameter maps for infants at preterm and term timepoints.

we performed a linear regression on each dataset and calculated the 95% confidence interval on the slope, to see whether the slope confidence interval included 0, which we will denote as 'not changing'. In the thalamus, the MD decreases, the FA and v_i increase and the ODI and v_{iso} do not change. In the cortex, the MD, FA and v_{iso} decrease while the ODI increases. The v_i does not change.

Discussion

The cortex

We observed the changes we predicted in the Hypothesis section in v_{iso} and ODI but not in v_i. Of the 7 longitudinal subjects, all demonstrated the trends in v_{iso} and ODI. These changes correspond to a reduction in FA over the same timescale. Thus changes in the FA correspond more closely with orientation dispersion than with v_i. Although there is an increasing cellular density during this period it does not appear to show in the v_i measurement. There may be other microstructural elements confounding the measurement, or the v_i may not be particularly sensitive to this change.

Although there was no significant evidence of an increase in v_i, looking at Fig. 7, infants b, c, g and h have the largest gestational ages at the term scans and higher v_i values. This suggests a non-linear change in the parameter, with a decrease preceding an increase. However, more subjects would be needed to support this assertion.

Thalamic GM

We predicted and observed an increase in the v_i for each pair of scans, indicating sensitivity to myelination status. While the ODI does not show evidence of change, the increase in v_i supports the hypothesis that the NODDI model is sensitive to the geometry of the surroundings. In this case, we interpret the increase in v_i as being caused, at least partially, by the myelin filling the extra-cellular space.

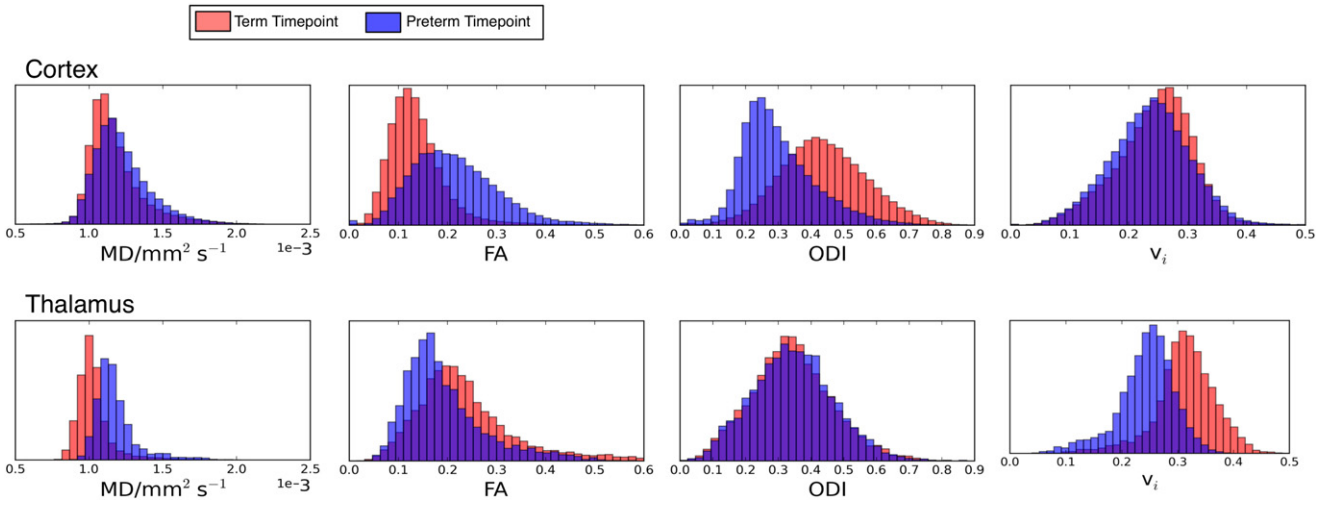

Fig. 6. Histograms of parameter values at the two time-points for the cortical grey matter. The y-axis represents the number of voxels (normalised so that the areas of preterm and term infants are equal). The trends and values for the parameters depend on the region.

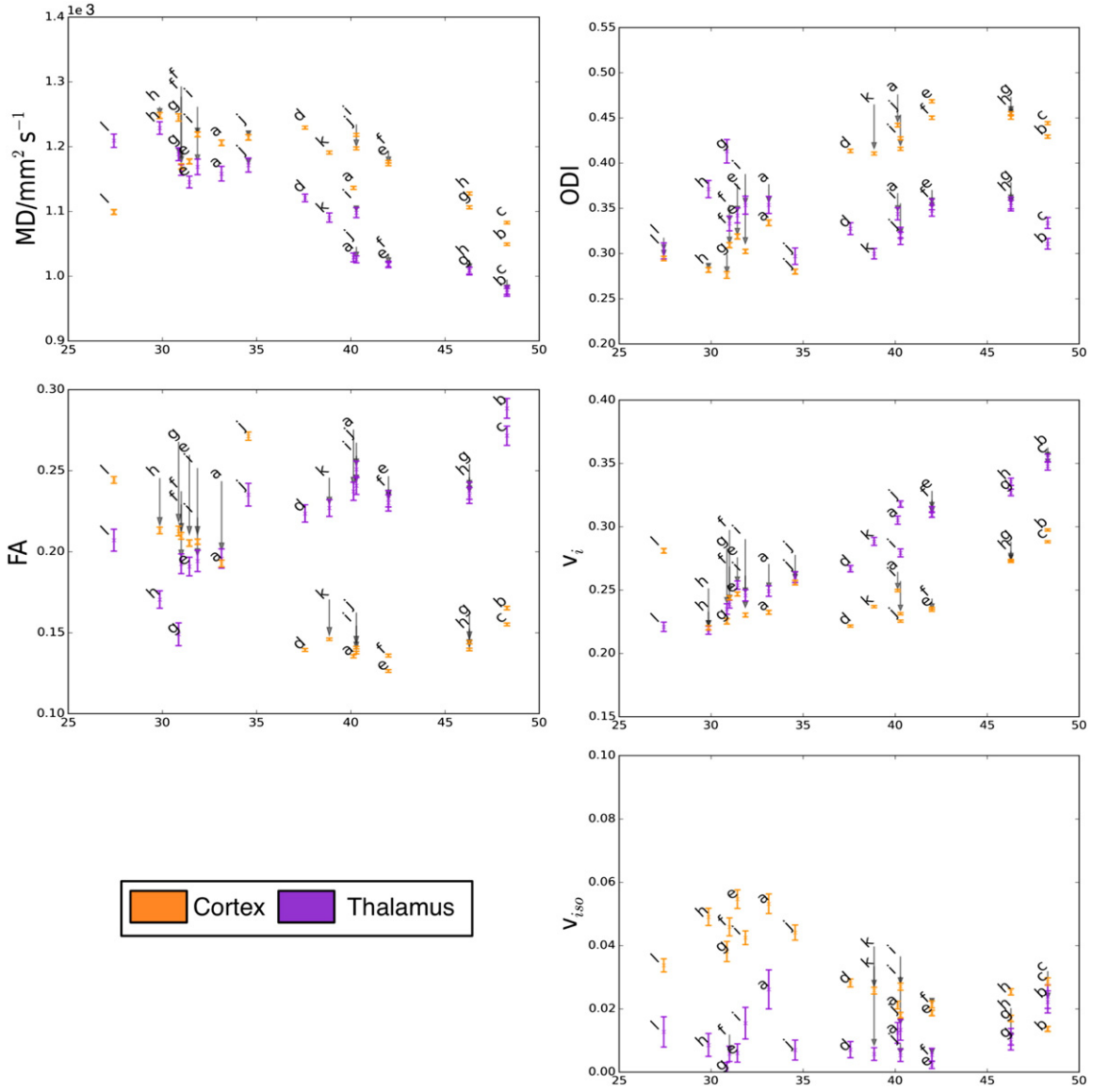

Fig. 7. For each infant, we plot the 95% confidence interval on the mean against gestational age for cortical and thalamic voxels. Datapoints are labelled with the letter of the infant (Table 1). The parameter changes over time agree with the trends in Fig. 6. The authors recommend viewing this diagram electronically for clarity.

Cross-sectional data

Combining the measurements from all subjects allows some of the trends to be shown more clearly (Fig. 7). In the thalamus, the trends are linear, as in Ball et al. (2012). We interpret the combination of NODDI and DTI parameters to show that the thalamus is myelinating during this time-period, with the differences being seen most clearly in the v_i values. The values in the cortex show some evidence of non-linearity, as in Ball et al. (2013), where the piecewise linear fit has a break at approximately 38 weeks for the FA measurements. From weeks 35–50 in our data, there is an increase in v_i. This may be related to the cellular density. This cross-sectional aspect is an area of future interest as we acquire more infants and controls.

Utility of the NODDI model in the preterm population

When interpreting DTI measures, similar combinations of FA and MD can be interpreted in differing ways depending on the anatomy. For example, high FA can represent a diverse array of microstructural conditions. The NODDI parameters, being compartments with biophysical inspiration, are more specific in their relation to the underlying microstructure.

In both the cortex and the thalamus, there are concurrent changes in the FA and in the MD. Both regions have a decreasing MD, which is a general feature of early brain maturation. The FA changes occur in the opposite direction for the cortex versus the thalamus. In the cortex, the ODI increases while the v_i's change does not significantly differ from 0. This suggests that the major changes occurring have something to do with geometry and a more complex microstructure. In the thalamus, the changes are reflected as an increase in v_i — which, in this case, could reflect a decrease in extra-cellular space due to the development of myelin. The parameter changes depend on the local tissue type as well as general maturational trends.

In terms of the practicalities of scanning infants, acquiring multiple shells of diffusion data in a suitable timeframe remains a technical challenge. The scans that we have presented in this work demonstrate a good compromise between image quality and scan duration. From Table 1 we can see that of the 12 subjects that we present data from, 7 of these had good data from both time-points. There were further two infants rejected because of brain abnormality. The cortical segmentation worked well in the T_1-weighted data. Although this requires more of the scans to go well, there is no practical way of segmenting in the diffusion images. There remain issues with the segmentation being moved to diffusion space, especially in dealing with susceptibility artefacts.

Limitations

In this study, we have presented data from 4 sets of twins. Twinning is a major cause of preterm birth and we did not analyse the twins as a separate sub-group. Data from twin pairs shows less variation than from unrelated individuals, which may reduce the generalisability of the results.

Although v_i seems to correlate with myelination status, much as with the DTI model, the parameters may not be specific to myelin alone. For example, the v_i may be affected by the packing of the fibres that may change independent of myelination. The water trapped in myelin cannot be directly imaged by DW-MRI and thus we are relying on the geometry of the diffusion to infer myelin indirectly. Thus, when interpreting results, it is still necessary to know the underlying biological processes.

In the NODDI model, we fixed the axial diffusion parameter at 2.00×10^{-3} mm^2 s^{-1} as in Kunz et al. (2014), in contrast to the adult value of 1.70×10^{-3} mm^2 s^{-1} from the original paper (Zhang et al., 2012). We believe that this value is representative for the cohort. In terms of its physical meaning, it represents the diffusivity along neurite tissue, which is different between adults and neonates — but also between preterm and term subjects. Preterm infants have higher diffusivities, so the choice of a constant value for both timepoints is a compromise. While in theory, the value could vary for each subject, this would add another parameter to the NODDI model and may reduce comparability between subjects. It would be an interesting avenue of future work to investigate the effects of varying the axial diffusivity on the volume fractions and ODI, albeit out of the scope of the current work.

Future work

Different areas of the cortex have different functional roles. Therefore, abnormalities of development in a given cortical region may manifest as associated functional defects at a later date. In addition to microstructural changes, the morphology of the cortex may also be different. In the future, we will combine morphology measurements with the diffusion data, as in Melbourne et al. (2013), in order to build a complete picture of perinatal growth. We will also investigate imaging correlates of the results of psychological testing in infancy.

Conclusions

In this study we have calculated NODDI parameters in the developing brain. We produced whole-brain maps of the parameters and analysed them on a region-of-interest basis. Using a multi-compartment diffusion model extends the work that has been performed using the DTI model. The thalamus and cortex show different trends in development, which relate to underlying differences in microstructural development. NODDI allows a more biologically-motivated interpretation of the diffusion data, which is important for defining robust developmental biomarkers in this cohort.

Acknowledgments

We would like to acknowledge UK registered charity Sparks (09UCL04), the EPSRC (EP/H046410/1, EP/J020990/1, EP/K005278), the MRC (MR/J01107X/1), the EU-FP7 project VPH-DARE@IT (FP7-ICT-2011-9-601055) and the National Institute for Health Research University College London Hospitals Biomedical Research Centre (NIHR BRC UCLH/UCL High Impact Initiative). NM receives part funding from the Department of Health's NIHR Biomedical Research Centre funding scheme at UCLH/UCL. We would also like to thank Dr. H. Zhang for his valuable thoughts and comments on the NODDI model.

Appendix A. Supplementary data

Supplementary data to this article can be found online at http://dx.doi.org/10.1016/j.neuroimage.2015.02.010.

References

Assaf, Y., Basser, P.J., 2005. Composite hindered and restricted model of diffusion (CHARMED) MR imaging of the human brain. NeuroImage 27 (1), 48–58 (August).
Bai, Y., Alexander, D.C., 2008. Model-based registration to correct for motion between acquisitions in diffusion MR imaging. IEEE International Symposium on Biomedical Imaging: From Nano to Macro. vol. 1–4, pp. 947–950.
Ball, G., Boardman, J.P., Rueckert, D., Aljabar, P., Arichi, T., Merchant, N., Gousias, I.S., Edwards, A.D., Counsell, S.J., 2012. The effect of preterm birth on thalamic and cortical development. Cereb. Cortex 22 (5), 1016–1024 (May).
Ball, G., Srinivasan, L., Aljabar, P., Counsell, S.J., Durighel, G., Hajnal, J.V., Rutherford, M.A., Edwards, A.D., 2013. Development of cortical microstructure in the preterm human brain. Proc. Natl. Acad. Sci. U. S. A. 110 (23), 9541–9546 (June).
Basser, P., 1995. Inferring microstructural features and the physiological state of tissues from diffusion-weighted images. NMR Biomed. 8, 334–344.
Basser, P.J., Mattiello, J., LeBihan, D., 1994. MR diffusion tensor spectroscopy and imaging. Biophys. J. 66, 259–267 (January).
Beck, S., Wojdyla, D., Say, L., Betran, A.P., Merialdi, M., Requejo, J.H., Rubens, C., Menon, R., Van Look, P.F.A., 2010. The worldwide incidence of preterm birth: a systematic review of maternal mortality and morbidity. Bull. World Health Organ. 88 (1), 31–38 (January).

Behrman, R., Butler, A., 2007. Preterm Birth: Causes, Consequences, and Prevention. Institute of Medicine (US) Committee on Understanding Premature Birth and Assuring Healthy Outcomes.
Bystron, I., Blakemore, C., Rakic, P., 2008. Development of the human cerebral cortex: Boulder Committee revisited. Nat. Rev. Neurosci. 9 (2), 110–122 (February).
Cardoso, M.J., Wolz, R., Modat, M., Fox, N.C., Rueckert, D., Ourselin, S., 2012. Geodesic information flows. In: Peters, T., Fichtinger, G., Martell, A. (Eds.), MICCAI 2012, Part II. LNCS vol. 15. Springer, Heidelberg, pp. 262–270.
Cardoso, M.J., Melbourne, A., Kendall, G.S., Modat, M., Robertson, N.J., Marlow, N., Ourselin, S., 2013. AdaPT: an adaptive preterm segmentation algorithm for neonatal brain MRI. NeuroImage 65, 97–108 (January).
Counsell, S.J., Zhang, H., Hughes, E., Steele, H., Tusor, N., Ball, G., Makropoulos, A., Alexander, D.C., Hajnal, J.V., Edwards, A.D., 2014. In vivo assessment of neurite density in the preterm brain using diffusion magnetic resonance imaging. International Society for Magnetic Resonance in Medicine. vol. 22, p. 1745.
Dekaban, A., 1954. Anatomical, developmental and pathological study development of the human thalamic nuclei. J. Comp. Neurol. 100, 63–97.
Dubois, J., Dehaene-Lambertz, G., Perrin, M., Mangin, J.F., Cointepas, Y., Duchesnay, E., Le Bihan, D., Hertz-Pannier, L., 2008. Asynchrony of the early maturation of white matter bundles in healthy infants: quantitative landmarks revealed noninvasively by diffusion tensor imaging. Hum. Brain Mapp. 29 (1), 14–27 (January).
Eaton-Rosen, Z., Melbourne, A., Orasanu, E., Modat, M., Cardoso, J., Bainbridge, A., Kendall, G.S., Robertson, N.J., Marlow, N., Ourselin, S., 2014a. Longitudinal measurement of the developing thalamus in the preterm brain using multi-modal MRI. Medical Image Computing and Computer-assisted Intervention: MICCAI. vol. II, pp. 276–283.
Eaton-Rosen, Z., Melbourne, A., Orasanu, E., Bainbridge, A., Kendall, G.S., Robertson, N.J., Marlow, N., Ourselin, S., 2014b. Cortical maturation in the preterm period revealed using a multi-component diffusion-weighted MR model. International Society for Magnetic Resonance in Medicine. vol. 22, p. 2014.
Gousias, I.S., Edwards, A.D., Rutherford, M.A., Counsell, S.J., Hajnal, J.V., Rueckert, D., Hammers, A., 2012. Magnetic resonance imaging of the newborn brain: manual segmentation of labelled atlases in term-born and preterm infants. NeuroImage 62 (3), 1499–1509 (September).
Greve, D.N., Fischl, B., 2009. Accurate and robust brain image alignment using boundary-based registration. NeuroImage 48 (1), 63–72 (October).
Hasegawa, M., Houdou, S., Mito, T., Takashima, S., Asanuma, K., Ohno, T., 1992. Development of myelination in the human fetal and infant cerebrum: a myelin basic protein immunohistochemical study. Brain and Development 14 (1), 1–6 (January).
Jones, D.K., Knösche, T.R., Turner, R., 2013. White matter integrity, fiber count, and other fallacies: the do's and don'ts of diffusion MRI. NeuroImage 73, 239–254 (June).
Kostović, I., Judas, M., 2010. The development of the subplate and thalamocortical connections in the human foetal brain. Acta Paediatr. 99 (8), 1119–1127 (August).
Kuklisova-Murgasova, M., Aljabar, P., Srinivasan, L., Counsell, S.J., Doria, V., Serag, A., Gousias, I.S., Boardman, J.P., Rutherford, M.A., Edwards, A.D., Hajnal, J.V., Rueckert, D., 2011. A dynamic 4D probabilistic atlas of the developing brain. NeuroImage 54 (4), 2750–2763 (February).
Kunz, N., Zhang, H., Vasung, L., O'Brien, K., 2014. Assessing white matter microstructure of the newborn with multi-shell diffusion MRI and biophysical compartment models. NeuroImage 96, 288–299 (August).
Le Bihan, D., 2003. Looking into the functional architecture of the brain with diffusion MRI. Nat. Rev. Neurosci. 4 (6), 469–480 (June).
Leemans, A., Jones, D.K., 2009. The B-matrix must be rotated when correcting for subject motion in DTI data. Magn. Reson. Med. 61 (6), 1336–1349 (June).
McKinstry, R.C., Mathur, A., Miller, J.H., Ozcan, A., Snyder, A.Z., Schefft, G.L., Almli, C.R., Shiran, S.I., Conturo, T.E., Neil, J.J., 2002. Radial organization of developing preterm human cerebral cortex revealed by non-invasive water diffusion anisotropy MRI. Cereb. Cortex 12 (12), 1237–1243.
Melbourne, A., Kendall, G.S., Cardoso, M.J., Gunny, R., Robertson, N.J., Marlow, N., Ourselin, S., 2013. Preterm birth affects the developmental synergy between cortical folding and cortical connectivity observed on multimodal MRI. NeuroImage 89, 23–34 (December).
Ment, L.R., Hirtz, D., Hüppi, P.S., 2009. Imaging biomarkers of outcome in the developing preterm brain. Lancet 8 (11), 1042–1055 (November).
Ourselin, S., Roche, A., Prima, S., Ayache, N., 2000. Block matching: a general framework to improve robustness of rigid registration of medical images. Medical Image Computing and Computer-assisted Intervention: MICCAIpp. 557–566.
Ourselin, S., Stefanescu, R., Pennec, X., 2002. Robust registration of multi-modal images: towards real-time clinical applications. Medical Image Computing and Computer-assisted Intervention: MICCAIpp. 140–147.
Partridge, S.C., Mukherjee, P., Henry, R.G., Miller, S.P., Berman, J.I., Jin, H., Lu, Y., Glenn, O.A., Ferriero, D.M., Barkovich, A.J., Vigneron, D.B., 2004. Diffusion tensor imaging: serial quantitation of white matter tract maturity in premature newborns. NeuroImage 22 (3), 1302–1314 (July).
Petrou, S., 2003. Economic consequences of preterm birth and low birthweight. BJOG 110, 17–23 (April).
Saigal, S., Doyle, L.W., 2008. An overview of mortality and sequelae of preterm birth from infancy to adulthood. Lancet 371 (9608), 261–269 (January).
Stanisz, G.J., Szafer, A., Wright, G.A., Henkelman, R.M., 1997. An analytical model of restricted diffusion in bovine optic nerve. Magn. Reson. Med. 37 (1), 103–111 (January).
Trivedi, R., Gupta, R.K., Husain, N., Rathore, R.K.S., Saksena, S., Srivastava, S., Malik, G.K., Das, V., Pradhan, M., Sarma, M.K., Pandey, C.M., Narayana, P.A., 2009. Region-specific maturation of cerebral cortex in human fetal brain: diffusion tensor imaging and histology. Neuroradiology 51 (9), 567–576 (September).
Volpe, J.J., 2009. Brain injury in premature infants: a complex amalgam of destructive and developmental disturbances. Lancet Neurol. 8 (1), 110–124 (January).
Wood, N.S., Marlow, N., Costeloe, K., Gibson, A.T., Wilkinson, A.R., 2000. Neurologic and developmental disability after extremely preterm birth. N. Engl. J. Med. 343 (6), 378–384.
Zhang, H., Hubbard, P.L., Parker, G.J.M., Alexander, D.C., 2011. Axon diameter mapping in the presence of orientation dispersion with diffusion MRI. NeuroImage 56 (3), 1301–1315 (June).
Zhang, H., Schneider, T., Wheeler-Kingshott, C.A., Alexander, D.C., 2012. NODDI: practical in vivo neurite orientation dispersion and density imaging of the human brain. NeuroImage 61 (4), 1000–1016 (July).